Electronic supplementary material

Pt-CoP/C as an alternative PtRu/C catalyst for direct methanol fuel cells

Jinfa Chang[a,d], Ligang Feng[b,*] Kun Jiang[c], Huaiguo Xue[b], Wen-bin Cai[c,*], Changpeng Liu[a] and Wei Xing[a,*]

[a] *State Key Laboratory of Electroanalytical Chemistry, Laboratory of Advanced Power Sources, Changchun Institute of Applied Chemistry, University of Chinese Academy of Sciences, Changchun 130022, P.R. China*

E-mail: xingwei@ciac.ac.cn

[b] *School of Chemistry and Chemical Engineering, Yangzhou University, Yangzhou, 225002, P.R. China.*

E-mail: ligang.feng@yzu.edu.cn

[c] *Shanghai Key Laboratory of Molecular Catalysis and Innovative Materials, Collaborative Innovation Center of Chemistry for Energy Materials, Department of Chemistry, Fudan University, Shanghai 200433. P.R. China.*

E-mail: wbcai@fudan.edu.cn

[d] *University of Chinese Academy of Sciences, Beijing 100039, PR China*

EXPERIMENTAL

Chemicals and materials

Sodium hypophosphite monohydrate (≥ 99.0%, $NaH_2PO_2 \cdot H_2O$), cobalt chloride hexahydrate (≥ 98.0%, $CoCl_2 \cdot 6H_2O$), hexachloroplatinic acid ($H_2PtCl_6 \cdot 6H_2O$) and methanol were purchased from Aldrich Chemical Co. (USA). Vulcan carbon powder XC-72 was purchased from Cabot Co. (USA). Commercial state-of-the-art Pt/C with 20 wt.% Pt loading (denoted as Pt/C-JM) and Commercial state-of-the-art PtRu/C with 20 wt.% Pt and 10 wt. % Ru loading (denoted as PtRu/C-JM) was purchased from Johnson Matthey Company. Nafion solution (5%) was purchased from Dupont Co. (USA). sulfuric acid (≥ 95.0%) and ethanol (≥ 99.7%) were purchased from Beijing Chemical Co. (China). All the chemicals were of analytical grade and used as received. Highly purified nitrogen (≥ 99.99%), oxygen (≥ 99.99%) and carbon monoxide (≥ 99.99%) were supplied by Changchun Juyang Co Ltd. Ultrapure water (resistivity：$\rho \geq 18$ $M\Omega cm^{-1}$) was used to prepare the solutions.

Preparation of CoP, CoP/C and Pt-CoP/C

CoP was prepared by a solid phase reaction method. A solid phase of 0.66 g $NaH_2PO_2 \cdot H_2O$ and 0.6 g $CoCl_2 \cdot 6H_2O$ was mechanically mixed in a quartz boat at room temperature. The precursor was directly heated to 600 °C and kept for 1 h in a flowing 30 mL min^{-1} N_2. Following cooling to room temperature in continued N_2 flow, the unsupported CoP was passivated in a 1.0 mol % O_2/N_2 mixture at 20 mL min^{-1} for 3 h.

A carbon-supported CoP was prepared by a new route. Typically, 0.529 g Vulcan XC-72 was incipiently impregnated with an aqueous solution of 0.6 g $CoCl_2$, followed by drying at 120 ℃ for 3h. Other steps are similar to prepare bulk CoP to obtain CoP/C-30% (30% representative wt. % of CoP in the hybrid support). Other compositions of CoP in hybrid support were also prepared and they were referred to as CoP/C-X% (X = 10, 20, 40, 50).

The platinum catalysts supported on CoP/C hybrid material with 5 wt. % Pt were prepared by microwave-assisted ethylene glycol reduction process. Briefly, 95 mg of CoP/C-X% support was ultrasonically dispersed in 100 ml of ethylene glycol to form a uniform suspension. Under stirring, a certain amount of H_2PtCl_6 solution (contain 5 mg Pt) was added to the suspension, and the pH of the suspension was adjusted to approximately 11.0 with 1.0 M NaOH solution. Then the suspension was placed and exposed in the middle of a microwave oven (LGMG-5021MW1, 2450 MHz) with 700 W with 90 s and cooled to room temperature naturally. At last, the suspension was filtered, washed and dried overnight at 80 °C in a vacuum oven to obtain the Pt-CoP/C-X% catalyst. The platinum catalyst supported on XC-72

(denoted as Pt/C-H) was prepared by the same method. The carbon supported PtCo catalyst (denoted as Pt-Co/C) was synthesized using a similar method except a certain amount of H_2PtCl_6 solution (containing 5 mg Pt) and $CoCl_2 \cdot 6H_2O$ (containing 5 mg Co) was added to the suspension; Carbon supported PtP catalyst (denoted as Pt-P/C) was synthesized using a similar method except a certain amount of H_2PtCl_6 solution (contain 5 mg Pt) and NaH_2PO_2 (the mole ratios of Pt : $H_2PO_2^-$ = 1:60) was added to the suspension. A state-of-art commercial Pt/C catalyst (denoted as Pt/C-JM, Johnson Matthey Company) was used for comparison as a baseline catalyst.

Physical characterizations

All X-Ray diffraction (XRD) measurements were performed with a PW1700 diffractometer (Philips Co.) using a Cu Kα (λ = 1.5405 Å) radiation source operating at 40 kV and 40 mA. A fine powder sample was grinded, then put into the glass slide and pressed to make a flat surface under the glass slide.

All transmission electron microscopy (TEM), scanning transmission electron microscopy (STEM), element mapping analysis and energy dispersive X-ray detector spectrum (EDX) measurements were conducted on a TECNAI G2 operating at 200 kV. Metal deposited CoP/C samples were sonicated and dispersed in EtOH and placed dropwise onto a holey carbon support grid for TEM observation.

All X-Ray photoelectron spectroscopy (XPS) measurements were carried out on a Kratos XSAM-800 spectrometer with an Al Kα radiation source.

Electrochemical measurements

All the electrochemical measurements were performed with an EG & G PARSTAT 4000 potentiostat/galvanostat (Princeton Applied Research Co., USA). The cells used were a conventional three-compartment electrochemical cell. The saturated calomel electrode (SCE, Hg/Hg_2Cl_2) were used as the reference electrodes. All of the potentials are relative to the SCE electrode. A Pt disk was used as a counter electrode with a surface area of 0.0314 cm^2. A glassy carbon thin film electrode (diameter d = 4 mm) was used as a working electrode.

All Cyclic Voltammetry measurements were carried out with respect to SCE in a 0.5 M H_2SO_4 electrolyte and purged with high-purity N_2 to remove dissolved oxygen. Electrochemical experiments of methanol oxidation were performed in 0.5 M H_2SO_4 containing a 1 M CH_3OH solution. All solution preparations were supplied by MilliQ water. All catalyst electrodes were cleaned by polishing with a 0. 05 μm alumina powder suspension (water) followed by ultrasonic cleaning in deionised water before use.

Electrochemical Pre-treatment

The catalyst ink was prepared by ultrasonically dispersing a mixture containing 5 mg of catalyst, 950 μL of ethanol and 50 μL of a 5 wt. % Nafion solution. Next, 5 μL of the catalyst ink was pipetted onto a pre-cleaned working electrode.

Before electrochemical measurements, adsorption/desorption of hydrogen on metal nanoparticles surface were evaluated in 0.5 M H_2SO_4. The electrode potential was scanned between -0.2 V and 1.0 V vs. SCE at 50 mV s^{-1} for surface cleaning. The cyclic voltammetry measurement was carried out until the steady voltammogram was obtained (about 10 cycles).

Cyclic Voltammetry Measurements

The activity of metal nanoparticles for methanol electro-oxidation was measured. The measurements were carried out at room temperature in 0.5 M H_2SO_4 and 1 M solution of methanol at potential range between -0.2 and 1.0 V vs SCE and at a potential sweep rate of 50 mV s^{-1}.

CO stripping

99.99% of CO was purged through the catalyst surface in the cells filled with 0.5 M H_2SO_4 electrolyte for 30 min while holding the working electrode at 0.2 V vs. SCE. Then the system was purged with N_2 for 30 min to remove non-adsorbed CO before the measurements were made. The CO stripping was performed in the potential of the range -0.2 ~ 1.0 V at a scan rate of 50 mV s^{-1}. The electrochemical surface areas (ECSA) and the tolerance to CO poisoning were estimated by the CO stripping test, assuming that the Coulombic charge required for the oxidation of the CO monolayer was 420 μC cm^{-2}.

Chronoamperometry measurements

To estimate the stability of the catalysts, the chronoamperometric (CA) experiments were performed in still 0.5 M H_2SO_4 and 1 M methanol solution at 0.5 V.

Electrochemical Impedance Measurements

The electrochemical impedance spectra (EIS) were recorded at the frequency range from 100 kHz to 10 mHz with 10 points per decade. The amplitude of the sinusoidal potential signal was 5 mV.

MEA Fabrication and Single-cell Performance Test

Nafion 117 (DuPont) was used as the proton exchange membranes and the pre-treatment of the Nafion membrane was accomplished by successively treating the membrane in 5 wt. % H_2O_2 solution at 80 ℃, distilled water at 80 ℃, 8 wt.% H_2SO_4 solution at 80℃ and then in distilled water at 80 ℃ again, for 30 min in each step.

Membrane electrode assemblies (MEAs) with a 9 cm^2 active cell area were fabricated using a 'direct paint' technique to apply the catalyst layer. The 'catalyst inks' were prepared by dispersing the catalyst nanoparticles into appropriate amounts of Millipore® water and a 5% recast Nafion® solution. Anode and cathode 'catalyst inks' were directly painted onto carbon paper (TGPH060, 20 wt.% PTFE, Toray). For all MEAs in this study, the cathode consisted of unsupported platinum black nanoparticles (27 m^2 g^{-1}, Johnson Matthey) at a standard loading of 4 mg cm^{-2}. The anode consisted of carbon supported Pt catalysts. A single

cell test fixture consisted of machined graphite flow fields with direct liquid feeds and gold plated copper plates to avoid corrosion (Fuel Cell Technologies Inc.). Hot-pressing was conducted at 140 ℃ and 10 atm for 90 s.

Six different anode catalysts were investigated in this study: (I) 5 wt. % Pt on Vulcan XC-72 (Pt/C-H), (II) 5 wt. % Pt-P on Vulcan XC-72 (Pt-P/C), (III) 5 wt. % Pt-Co on Vulcan XC-72 (Pt-Co/C), (IV) 5 wt. % Pt on CoP@Vulcan XC-72 (Pt-CoP/C-30%), (V) 5 wt. % commercial Pt/C (Pt/C-JM). The anode Pt catalyst loading of the (I)~(V) was 0.3 mg cm^{-2}. (VI) 20 wt. % commercial Pt/C (Pt/C-JM) and the loading of Pt was 1.2 mg cm^{-2}.

The MEA was fitted between two graphite plates with a punctual flow bed on machined graphite. The polarization curves were obtained using a Fuel Cell Test System (Arbin Instrument Corp.) under the operation conditions of 60 ℃. High purity O_2 (99.99 %) is applied as the oxidant at 200 ml /min as the cathode atmosphere and 1 M methanol as the reactant feed at the anode side at 2.0 ml/min. Both sides are under ambient pressure. The steady-state polarization curve was measured by recording the cell potential for 1 min from the circuit voltage under constant current density.

***In situ* EC-ATR-IR Measurements**

The ATR-IR measurement was run on a Pt-based/C catalyst layer covered on Au film chemically deposited on the basal plane of a hemicylindrical Si prism using a Varian 3100 FT-IR Excalibur spectrometer equipped with an MCT detector, at a spectral resolution of 4 cm^{-1} with unpolarized IR radiation at an incidence angle of ca. 65°. 50 μL of catalyst ink was transferred onto an electrochemically polished Au film via a pipette. All the spectra are shown in the absorbance unit as -log (I/I_0), where I and I_0 represent the intensities of the reflected radiation of the sample and reference spectra, respectively. Experimental details including chemical deposition of the Au films, preparation of the catalyst ink and the catalyst overlayer on Au films, setup of the ATR cell etc., can be found elsewhere [1].

Supporting Tables and Figures

Table S1 Electrochemical surface area (ECSA) estimation from CO stripping experiment and peak potential for CO stripping for the different Pt-based and PtRu-based catalysts in 0.5 M H_2SO_4 with a scanning rate of 50 mV s^{-1}.

sample	ECSA (m^2 g^{-1})	peak potential (V)
Pt-CoP/C-10%	56.30	0.61
Pt-CoP/C-20%	65.22	0.61
Pt-CoP/C-30%	81.52	0.58
Pt-CoP/C-40%	76.15	0.58
Pt-CoP/C-50%	69.98	0.58
PtCo/C	80.23	0.61
PtP/C	74.48	0.58
Pt/C-JM	78.47	0.58
Pt/C-H	77.07	0.62
PtRu/C-JM	81.18	0.36
PtRu/C-H	68.04	0.39

Table S2 Mass activity and specific activity expressed as the positive scan peak current for all Pt/C catalysts in 1.0 M CH_3OH and 0.5 M H_2SO_4.

Sample	Mass Activity (mA mg^{-1}_{Pt})		Specific Activity (mA cm^{-2})	
	peak	@ 0.6 V vs.SCE	peak	@ 0.6 V vs.SCE
Pt-CoP/C-10%	827.19	826.02	1.47	1.46
Pt-CoP/C-20%	1191.25	1179.56	1.83	1.80
Pt-CoP/C-30%	1706.41	1608.86	2.09	1.96
Pt-CoP/C-40%	1465.31	1381.58	1.92	1.82
Pt-CoP/C-50%	989.53	977.53	1.42	1.41
Pt-Co/C	463.16	460.81	0.58	0.57
Pt-P/C	661.59	656.77	0.89	0.88
Pt/C-JM	303.43	295.40	0.39	0.37
Pt/C-H	242.42	239.41	0.32	0.31

Table S3 Maximum power density in DMFC use of Pt-CoP/C (30%) catalyst as anode compared with others.

Samples	Methanol concentration / M	Test temperature / ℃	noble loading / mg cm^{-2}	Mass activity / mW mg^{-1}	Area activity / mW cm^{-2}	Ref.
Pt-CoP/C-30%	2	30	2	62.4	124.8	This work
		50		72.1	144.2	
		70		88.5	177	
PtRu black (1:1)	2	90	2	90	180	2
PtRu/NCNT-GHN	2	30	7	6.1	43	3
		60		17.2	120.4	
		90		27.9	195.1	
Pt-Ru/BDDNP	1	80	4	13.8	55	4
PtRu Black-JM	2	25	4	2.4	9.5	5
		40		3.8	15.0	
		55		5.0	20.1	
PtRu/C-JM	2	65	2.5	13.2	33	6
PtRu alloy	2	30	3	16	48	7
		50		33	99	
		70		54	162	
PtRu/TECNF	2	80	0.58	84.5	49	8
PANI/PtRu/C	2	80	4	24	96	9
PtRu/C/Nafion/PVA [illegible]	4	25	2	22	44	10
PtRu/Porous MPL and [illegible]	3	25	2	21.8	43.7	11
PtRu/MCC-SBA-15(1/3)	1	70	4.3	3.0	13	12
PtRu/C-JM(20%:10%)	1	75	2	33	66	13
PtRu/XC-72(30%:15%)	1	75	2	79.5	159	14
PtRu/C-JM(30%:15%)				68	136	
PtRu black			4	34.5	138	
PtRu black(JM)				33.5	134	
PtRu/carbon nanofibers (70%)	1	30	3	20	60	15
		40		25	75	
		50		33.3	100	

		60		41	123	
		70		46	138	
PtRu/MWCNTs	2	70	2.1	26	54.6	16
PtRu/C+20%IrO_2	2	60	2	11.5	23	17
PtRu/C	2	80	3	26	78	18
PtRu/CNF(Platelet)	2	30	5	7.6	38	19
		60		18	90	
		90		25.6	128	
PtRu/C-SA	1	80	7.5	14.7	110	20
PtRu/MC	1	30	1.5	26	39	21
PtRuMo/CNTs	2	60	2	30.6	61.3	22
PtRu/Vulcan XC	2	30	3	14	42	23
		70		41.3	124	
PtRu/C(E-TEK)		30		35.3	46	
		70		45.7	137	
PtRu/HCMS		30		26.6	80	
		70		71.3	214	
PtRu	2	70	5	22	160	24
PtRuNiRh				36	180	
PtRu/C(house-made)20%	1	70	2.5	17.6	44	25
PtRu/C(E-TEK)20%				16.8	42	
PtRu/Ordered Porous Carbons	2	30	3	19.3	58	26
		70		55.7	167	
PtRu/C(20%:15%)	2	80	3	26	78	27
PtRu(1:1)/MWCNT	2	70	15.2	2.1	32	28
Pt-Ni2P/C-30%	1	60	1	65	65	29

CoP/C-30%

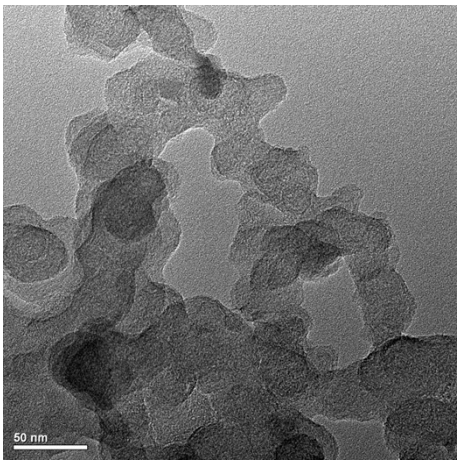

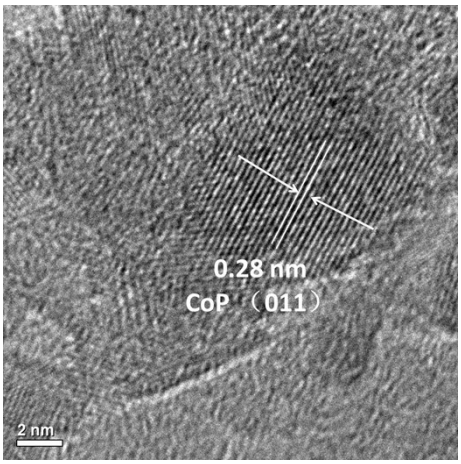

Pt-Co/C

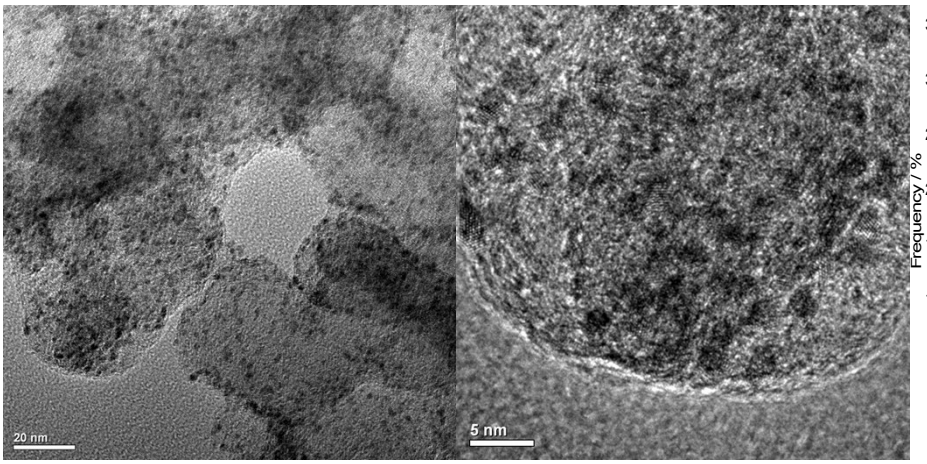

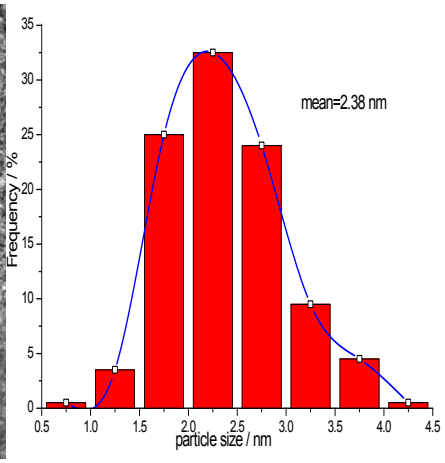

Pt-P/C

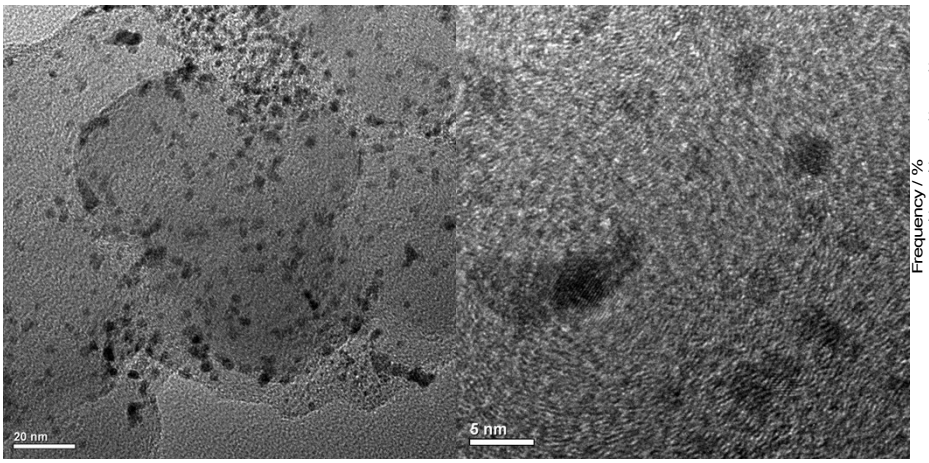

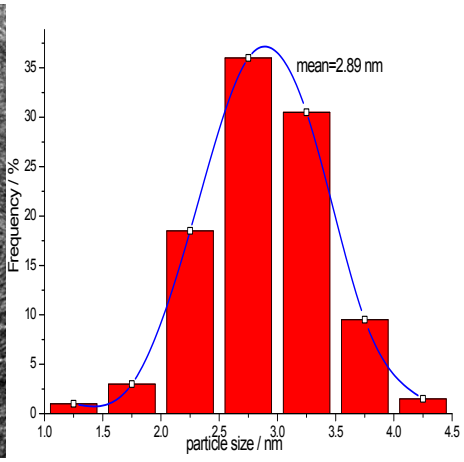

Pt/C-JM

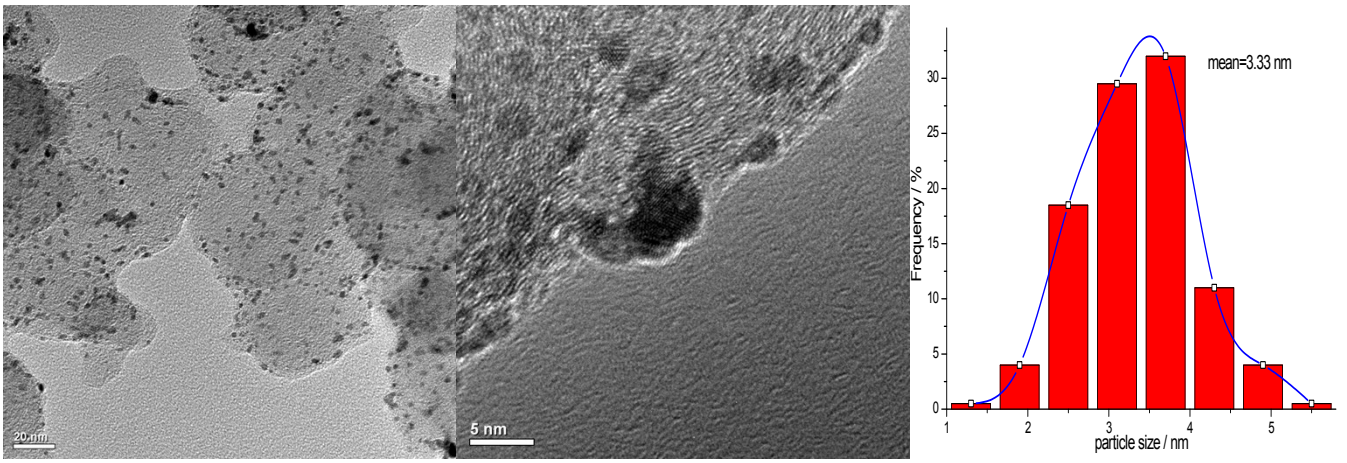

Pt/C-H

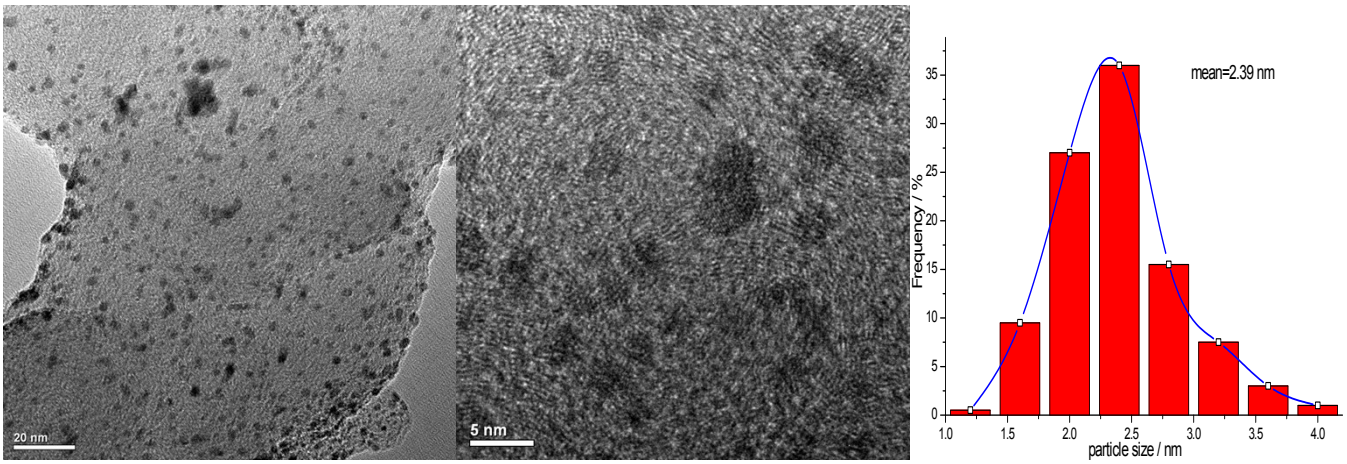

Figure S1. Typical TEM, HR-TEM images and the size distribution of Pt-Co/C, Pt-P/C, Pt/C-JM and Pt/C-H catalysts.

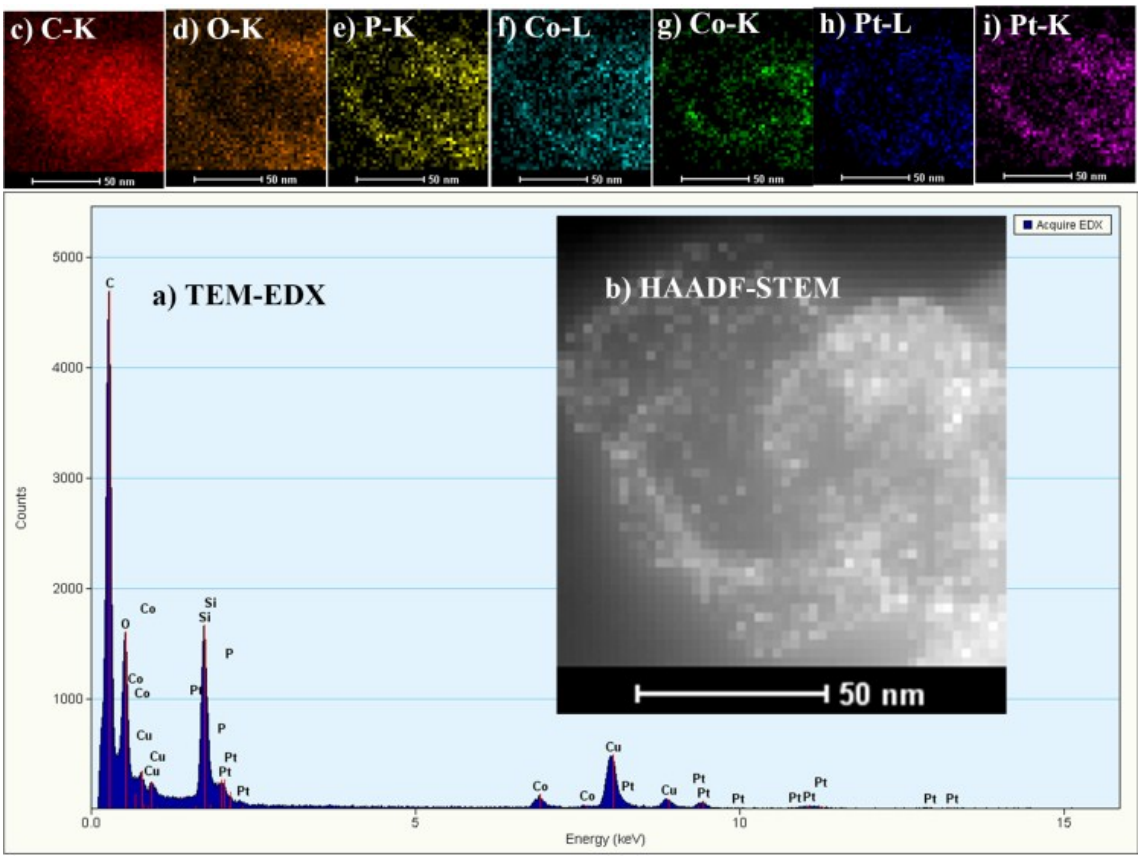

Fig. S2 (a) EDX, (b) STEM, (c-i) Elemental mapping images of the Pt-CoP/C-30% catalyst.

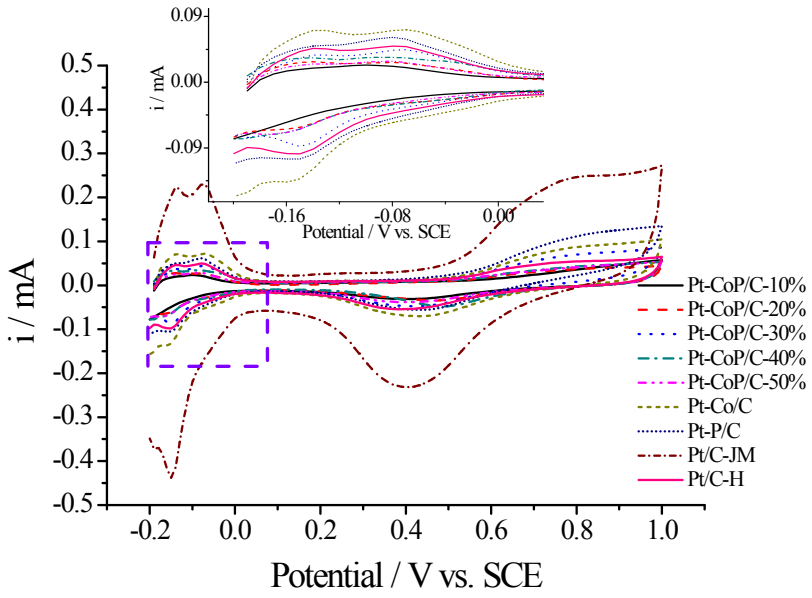

Fig. S3 Cyclic voltammograms of the Pt-CoP/C-10%, Pt-CoP/C-20%, Pt-CoP/C-30%, Pt-CoP/C-40%, Pt-CoP/C-50%, Pt-Co/C, Pt-P/C, Pt/C-JM and Pt/C-H catalysts in N_2-saturated 0.5 M H_2SO_4 with a scanning rate of 50 mV s^{-1}. Pt/C-JM with 20% $_{Pt}$ loading, and other samples with 5% $_{Pt}$ loading.

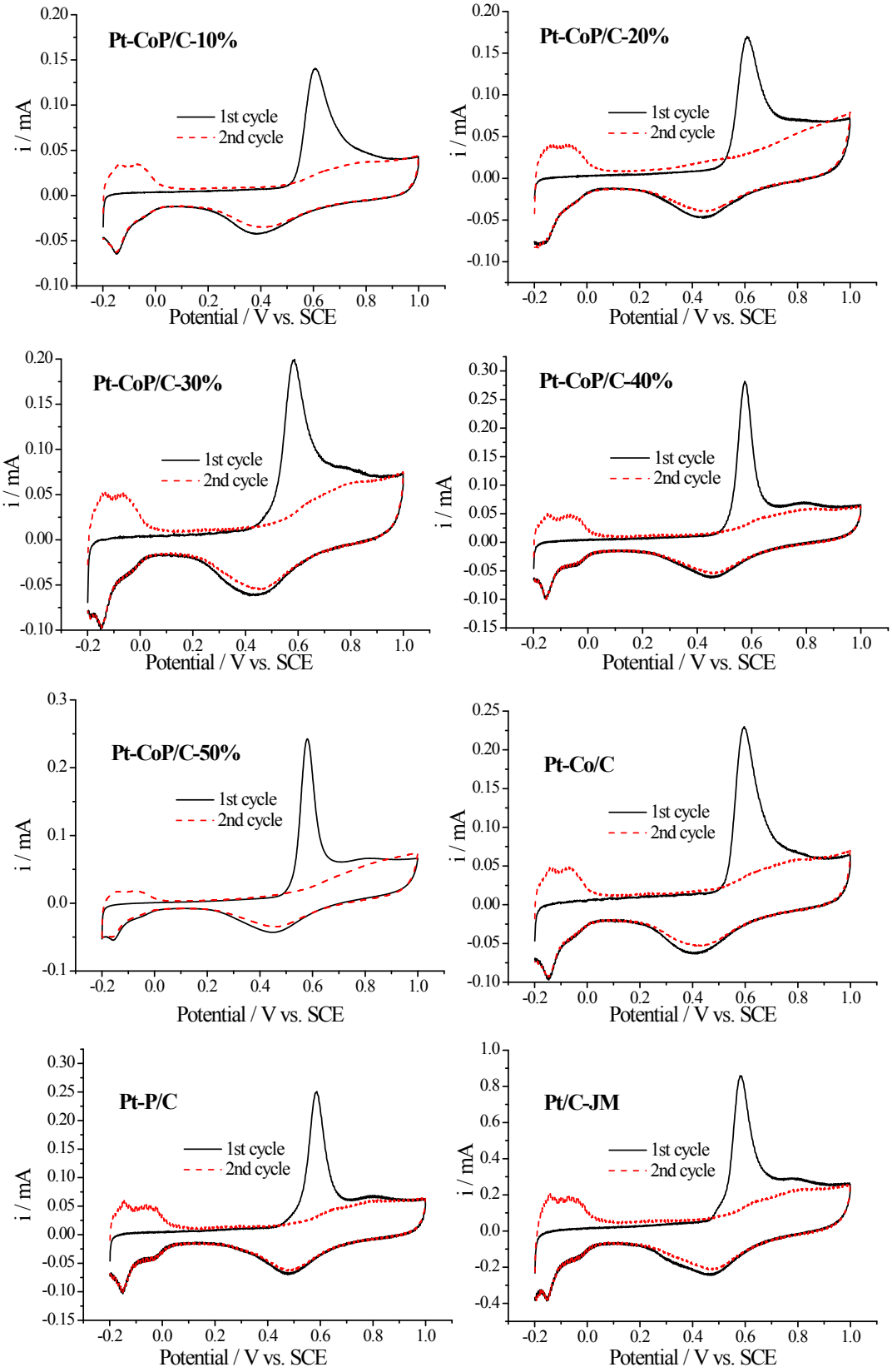
Pt-CoP/C-10%
Pt-CoP/C-20%
Pt-CoP/C-30%
Pt-CoP/C-40%
Pt-CoP/C-50%
Pt-Co/C
Pt-P/C
Pt/C-JM
1st cycle
2nd cycle
i / mA
Potential / V vs. SCE

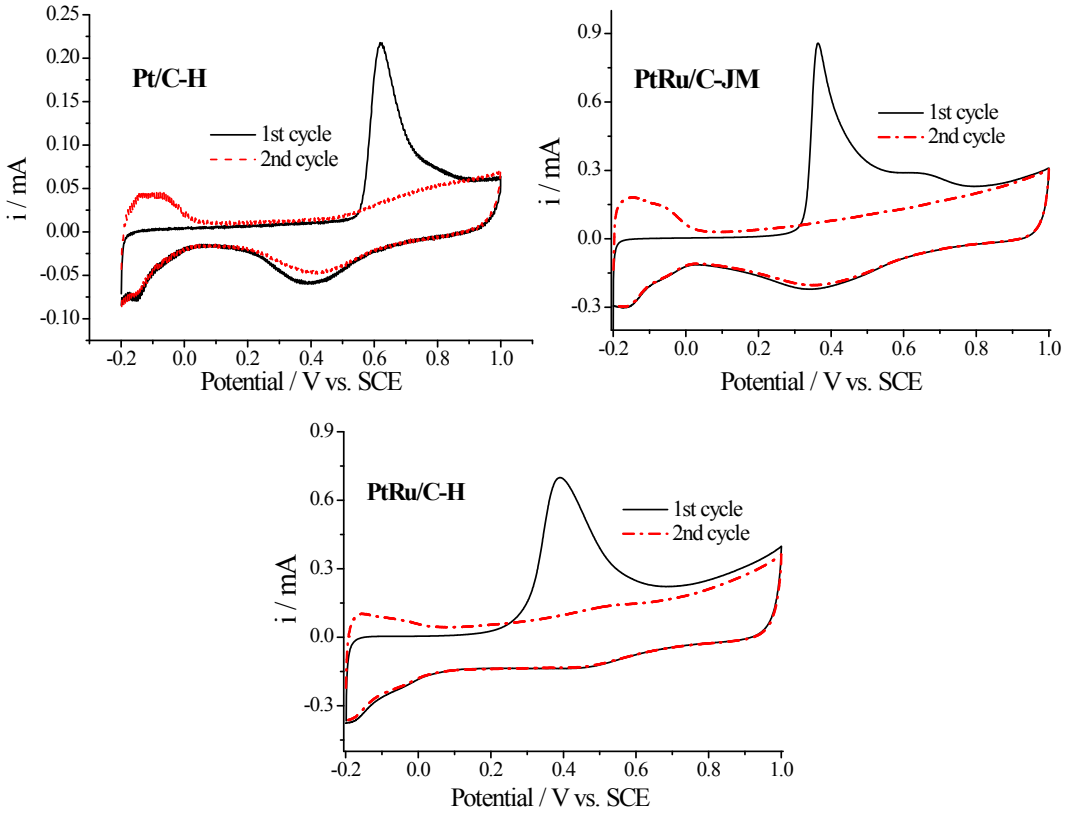

Fig. S4 CO stripping curves of the Pt-CoP/C-10%, Pt-CoP/C-20%, Pt-CoP/C-30%, Pt-CoP/C-40%, Pt-CoP/C-50%, Pt-Co/C, Pt-P/C, Pt/C-JM, Pt/C-H, PtRt/C-JM and PtRu/C-H catalysts in 0.5 M H_2SO_4 with a scanning rate of 50 mV s^{-1}.

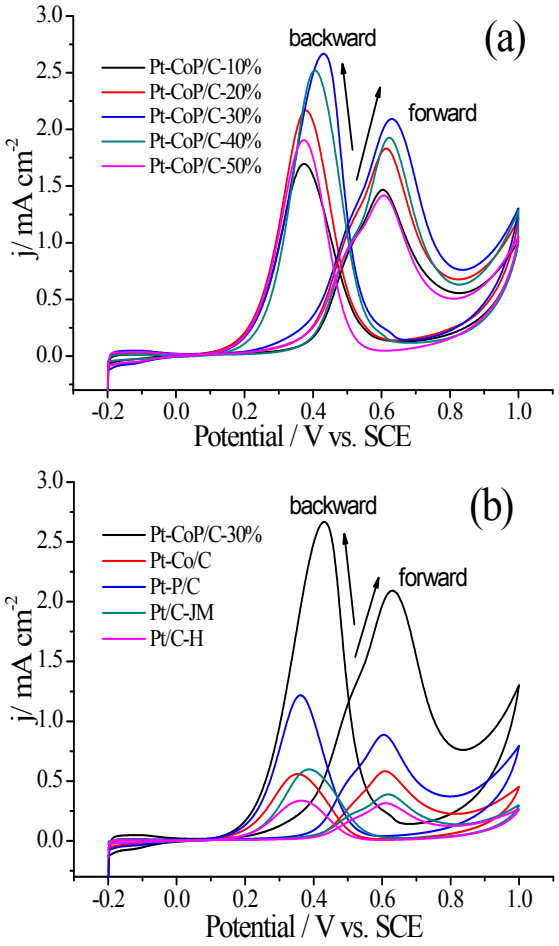

Fig. S5 (a) Cyclic voltammograms of the Pt-CoP/C catalysts with various loading of CoP in H_2SO_4 (0.5 M) containing CH_3OH (1.0 M). (b) Cyclic voltammograms of the Pt-CoP/C-30%, Pt-Co/C, Pt-P/C, Pt/C-JM and Pt/C-H catalysts in N_2-saturated H_2SO_4 (0.5 M) containing CH_3OH (1.0 M).

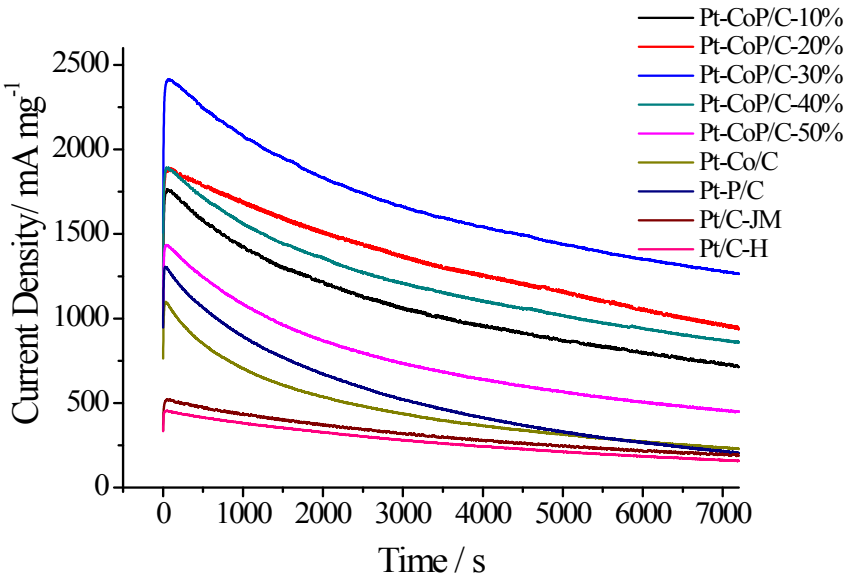

Fig. S6 CA curves for different Pt-based catalysts at 0.5 V for 7200 s in N_2-saturated 0.5 M H_2SO_4 solution containing 1.0 M CH_3OH.

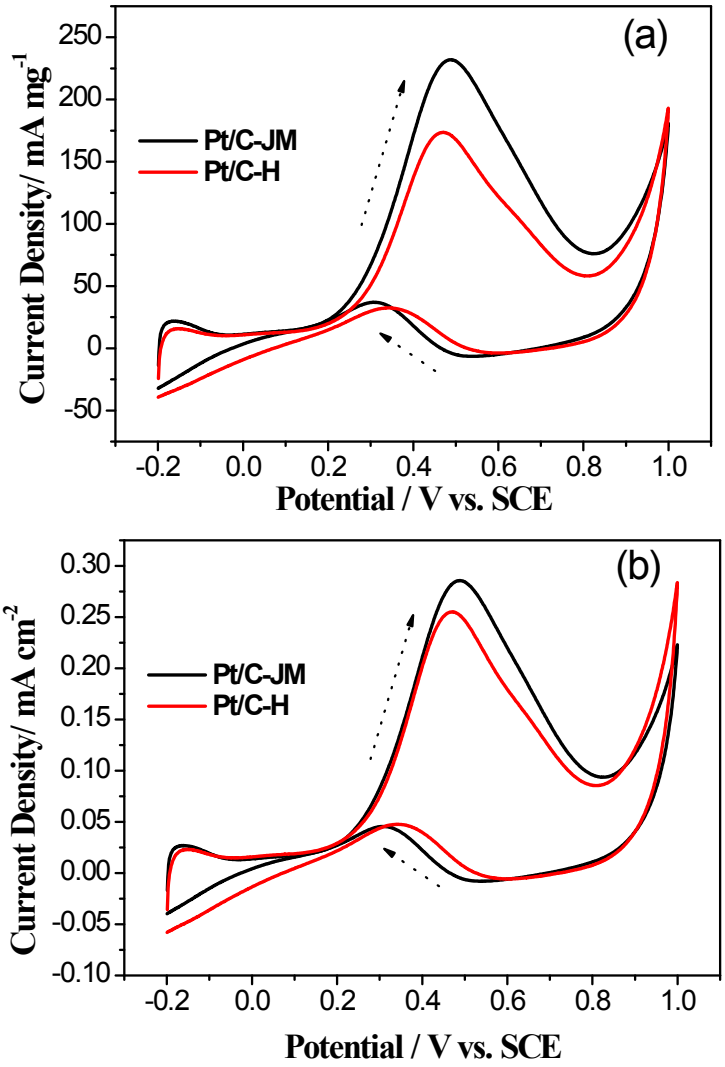

Fig. S7 The mass activity (a) and the specific activity (b) of PtRu/C-JM and PtRu/C-H catalysts in N_2-saturated H_2SO_4 (0.5 M) containing CH_3OH (1.0 M) at a scan rate of 50 mV dec^{-1}, the loading of the catalyst was 0.199 mg cm^{-2} including the carbon.

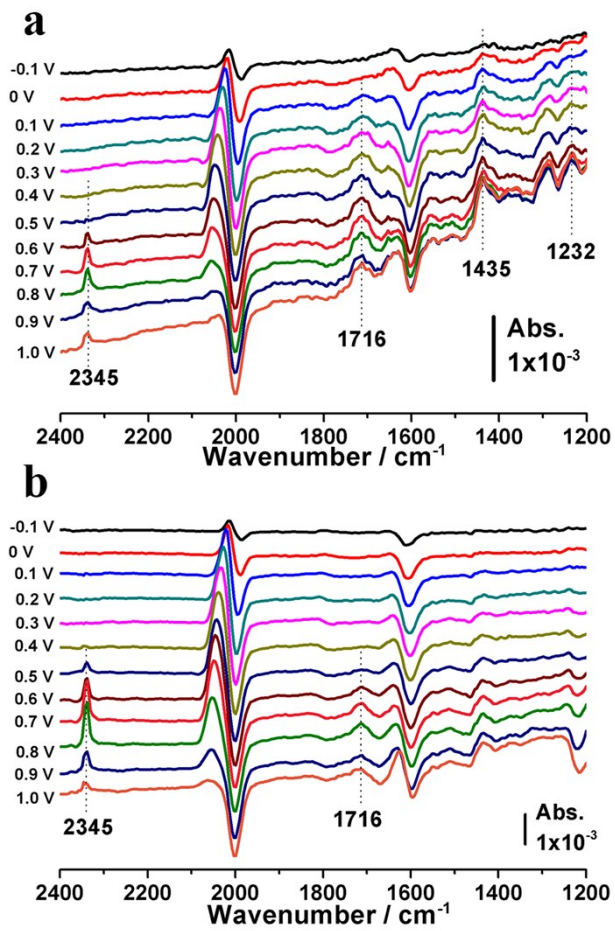

Fig. S8 The multi-step ATR-SEIRA spectra on the Pt/C-JM (a) and the Pt-CoP/C (b) electrodes. Reference spectrum was taken at -0.2 V (vs. SCE).

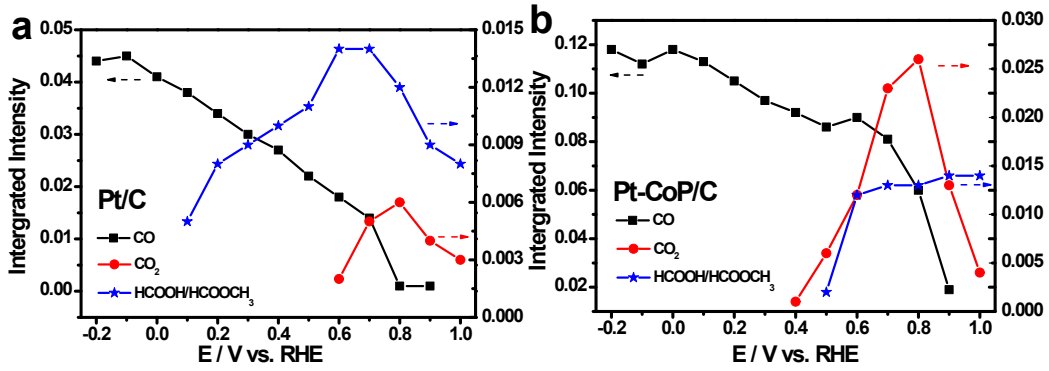

Fig. S9 Potential-dependent band intensities evolution for CO_{ad}, CO_2 and $HCOOH/HCOOCH_3$ species without normalization over Pt/C-JM (a) and Pt-CoP/C (b) catalysts, respectively.

Since the CO band intensities on both Pt and Pt-CoP surfaces are much higher than the CO_2 and $HCOOH/HCOOCH_3$ band intensities, we normalized the CO band intensity separately as shown in the left y axis in Fig. 7c and 7d, and normalized the CO_2 and $HCOOH/HCOOCH_3$ band intensities together in the right y axis. In all the cases, the largest band intensity for CO or CO_2/$HCOOH/HCOOCH_3$ was set to be 1.0, respectively. The absolute band intensities recorded on Pt/C and Pt-CoP/C was shown in Fig. S9, in which the interfacial species evolution is similiar to that in Fig. 7, i.e., the increase in the full oxidation product CO_2 and the decrease in partial oxidation product $HCOOH/HCOOCH_3$ are observed on Pt-CoP/C catalyst as compared to that on Pt/C catalyst. Notably, the more CO_{ad} species generated on Pt-CoP/C could arise from a more facile dissociation of methanol over the low potential region as compared to that on Pt/C, but this species can also be readily converted to CO_2 at the potential of 0.4 V on Pt-CoP/C, or, ca. 200 mV negative of the onset potential on Pt/C, as indicated in Fig. S9. Although a faster decay of CO species is seen on Pt/C with potential, it is accompanied by a more facile formation of the partial oxidation product $HCOOH/HCOOCH_3$. The selective oxidation of methanol to CO_2 on Pt-CoP/C enhances the electrocatalytic current.

In summary, these potential-dependent interfacial species evolution provides molecular insights that the introduction of CoP component promotes the direct oxidation pathway of CH_3OH to CO_2, giving rise to its enhanced electrocatalytic activity and fuel cell performance.

References

1. K. Jiang, K. Xu, S. Zou and W. B. Cai, *J. Am. Chem. Soc.*, 2014, **136**, 4861-4864.
2. D. Sebastián, V. Baglio, A. S. Aricò, A. Serov and P. Atanassov, *Applied Catalysis B: Environmental*, 2016, **182**, 297-305.
3. R. Lv, T. Cui, M.-S. Jun, Q. Zhang, A. Cao, D. S. Su, Z. Zhang, S.-H. Yoon, J. Miyawaki, I. Mochida and F. Kang, *Advanced Functional Materials*, 2011, **21**, 999-1006.
4. L. La-Torre-Riveros, R. Guzman-Blas, A. E. Méndez-Torres, M. Prelas, D. A. Tryk and C. R. Cabrera, *ACS Applied Materials & Interfaces*, 2012, **4**, 1134-1147.
5. Y. Wang, G. Liu, M. Wang, G. Liu, J. Li and X. Wang, *International Journal of Hydrogen Energy*, 2013, **38**, 9000-9007.
6. Z. Jiang, Y. Shi, Z.-J. Jiang, X. Tian, L. Luo and W. Chen, *Journal of Materials Chemistry A*, 2014, **2**, 6494-6503.
7. S.-A. Lee, K.-W. Park, J.-H. Choi, B.-K. Kwon and Y.-E. Sung, *J Electrochem Soc*, 2002, **149**, A1299-A1304.
8. Y. Ito, T. Takeuchi, T. Tsujiguchi, M. A. Abdelkareem and N. Nakagawa, *Journal of Power Sources*, 2013, **242**, 280-288.
9. M. Zhiani, H. Gharibi and K. Kakaei, *Journal of Power Sources*, 2012, **210**, 42-46.
10. P. Chen, H. Wu, T. Yuan, Z. Zou, H. Zhang, J. Zheng and H. Yang, *Journal of Power Sources*, 2014, **255**, 70-75.
11. Q. Huang, J. Jiang, J. Chai, T. Yuan, H. Zhang, Z. Zou, X. Zhang and H. Yang, *Journal of Power Sources*, 2014, **262**, 213-218.
12. J. M. R. Gallo, G. Gatti, A. Graizzaro, L. Marchese and H. O. Pastore, *Journal of Power Sources*, 2011, **196**, 8188-8196.
13. J. Liu, Z. h. Zhou, X. Zhao, Q. Xin, G. Sun and B. l. Yi, *Phys. Chem. Chem. Phys.*, 2004, **6**, 134–137.
14. J. Guo, G. Sun, S. Shiguo, Y. Shiyou, Y. Weiqian, Q. Jing, Y. Yushan and X. Qin, *J. Power Sources*

2007, **168**, 299-306.

15. S. Kang, S. Lim, D.-H. Peck, S.-K. Kim, D.-H. Jung, S.-H. Hong, H.-G. Jung and Y. Shul, *Int. J. Hydrogen Energy* 2012, **37**, 4685-4693.
16. J. Prabhuram, T. S. Zhao, Z. X. Liang and R. Chen, *Electrochimica Acta*, 2007, **52**, 2649-2656.
17. V. Baglio, D. Sebastián, C. D'Urso, A. Stassi, R. S. Amin, K. M. El-Khatib and A. S. Aricò, *Electrochimica Acta*, 2014, **128**, 304-310.
18. W. Xu, T. Lu, C. Liu and W. Xing, *The Journal of Physical Chemistry B*, 2005, **109**, 14325-14330.
19. M. Tsuji, M. Kubokawa, R. Yano, N. Miyamae, T. Tsuji, M.-S. Jun, S. Hong, S. Lim, S.-H. Yoon and I. Mochida, *Langmuir*, 2006, **23**, 387-390.
20. M. Carmo, M. Brandalise, A. O. Neto, E. V. Spinacé, A. D. Taylor, M. Linardi and J. G. Rocha Poço, *International Journal of Hydrogen Energy*, 2011, **36**, 14659-14667.
21. M. M. Bruno, M. A. Petruccelli, F. A. Viva and H. R. Corti, *International Journal of Hydrogen Energy*, 2013, **38**, 4116-4123.
22. S. Chen, F. Ye and W. Lin, *International Journal of Hydrogen Energy*, 2010, **35**, 8225-8233.
23. G. S. Chai, S. B. Yoon, J. H. Kim and J. S. Yu, *Chem Commun (Camb)*, 2004, DOI: 10.1039/b412747c, 2766-2767.
24. K.-W. Park, J.-H. Choi, S.-A. Lee, C. Pak, H. Chang and Y.-E. Sung, *J. catal.*, 2004, **224**, 236-242.
25. J. W. Guo, T. S. Zhao, J. Prabhuram, R. Chen and C. W. Wong, *Electrochimica Acta*, 2005, **51**, 754-763.
26. G. S. Chai, S. B. Yoon, J.-S. Yu, J.-H. Choi and Y.-E. Sung, *J. Phys. Chem. B*, 2004, **108**, 7074-7079.
27. W. Xu, T. Lu, C. Liu and W. Xing, *J. Phys. Chem. B*, 2005, **109**, 14325-14330.
28. J. Prabhuram, T. S. Zhao, Z. K. Tang, R. Chen and Z. X. Liang, *J. Phys. Chem. B*, 2006, **110**, 5245-5252.
29. J. Chang, L. Feng, C. Liu, W. Xing and X. Hu, *Energy Environ. Sci.*, 2014, **7**, 1628-1632.